

Wide-angle pion- $\Delta(1232)$ photoproduction

P. Kroll

Fachbereich Physik, Universität Wuppertal, D-42097 Wuppertal, Germany

Abstract

High-energy wide-angle photoproduction of $\pi\Delta$ final states is investigated within the handbag mechanism to twist-3 accuracy. In this approach the process amplitudes factorize in a hard partonic subprocess and in form factors which represent $1/x$ -moments of $p - \Delta$ transition generalized parton distributions (GPDs) at zero skewness. The subprocess, calculated to twist-3 accuracy, is the same as in pion photoproduction. The $p - \Delta$ GPDs are related to the proton-proton GPDs exploiting large- N_C results. The proton-proton GPDs as well as the twist-2 and twist-3 pion distribution amplitudes appearing in the subprocess are taken from other work. Reasonable agreement with experiment is found in this almost parameter-free analysis.

1 Introduction

Factorization properties of QCD allow to calculate inclusive and exclusive scattering processes. For exclusive processes, in particular, there are two kinematical regions in which factorization properties hold. On the one hand this is the generalized Bjorken region of large photon virtualities, Q^2 , large energies in the photon-nucleon center-of-mass system (c.m.s.) and fixed Bjorken- x but small Mandelstam $-t$ ($-t \ll Q^2$). In this kinematical region it has been shown [1, 2] that the process amplitudes are represented as a convolution of hard perturbatively calculable partonic subprocess and soft hadronic matrix elements parameterized as GPDs. There are many applications of this theoretical concept as for instance deeply virtual Compton

scattering or meson production, see for instance the reviews [3, 4]. The other kinematical region in which factorization applies, is the wide-angle region, i.e. the region where all three Mandelstam variables, s , $-t$ and $-u$, are large. Here the process amplitudes factorize in hard partonic subprocesses and soft form factors representing $1/x$ -moments of GPDs. This so-called handbag mechanism has been applied to wide-angle Compton scattering [5, 6] and photoproduction of pseudoscalar mesons [7, 8]. It also applies to electroproduction of mesons provided $Q^2 \ll -t$ [9]. Lack of data prevented further applications as for instance photoproduction of vector mesons.

Both these classes of hard exclusive processes, the deeply virtual as well as the wide-angle ones, are in a sense complementary. In the deeply-virtual region the GPDs are probed at small $-t$, typically less than 1 GeV^2 while in the wide-angle region the GPDs are examined at large $-t$. The knowledge of the large $-t$ behavior of the GPDs is important for studying the impact parameter distribution of partons inside the proton. As shown by Burkardt [10] the impact-parameter distribution of the partons is obtained from a Fourier transform of zero-skewness GPDs. The impact parameter is canonically conjugated to the momentum transfer from the initial to the final baryon. The square of the momentum transfer is the Mandelstem t . Obviously, for a reliable Fourier transform knowledge of the GPDs is required in a fairly large range of t , well beyond 1 GeV^2 .

Recently the interest in transition GPDs has strongly grown both experimentally and theoretically [11]. Besides baryon octet-octet transitions also octet-decuplet transitions and particularly $p - \Delta$ ones are of interest. Data relevant for the latter transition GPDs are scarce up to now. In the deeply virtual region only the beam spin asymmetry has been measured by the CLAS collaboration [12]. There is also a theoretical study of the $\pi^- \Delta^{++}(1232)$ electroproduction cross section in the generalized Bjorken regime [13]. The $p - \Delta$ transition GPDs are fixed in the large- N_C limit where relations between the $p - \Delta$ and the proton-proton GPDs hold [3, 14]. Here, in this article, wide-angle photoproduction of $\pi\Delta$ final states will be investigated. This process has been measured in the wide-angle region at high energies at SLAC [15] long ago. The calculation of wide-angle $\pi\Delta$ photoproduction goes along the same line as pion photoproduction [8]: the partonic subprocess is identical and has been calculated in [8] to twist-3 accuracy and leading-order of perturbative QCD. The transition GPDs are fixed in the large- N_C limit as in [13]. Thus, the $\pi\Delta$ photoproduction cross section can be calculated almost free of parameters and as will be shown in the following, reasonable

agreement with experiment is found.

The plan of the paper is as follows: In the next section the handbag mechanism for wide-angle photoproduction will be introduced. In Sect. 3 the subprocess and in Sect. 4 the GPDs in the large- N_C limit will be discussed. The results for the photoproduction cross section will be presented in Sect. 5 and compared to experiment. The paper will end with a summary.

2 The handbag mechanism for wide-angle photoproduction

Here, in this article, the process

$$\gamma(q, \mu) p(p, \nu) \rightarrow \pi(q', 0) \Delta(p', \nu') \quad (1)$$

will be investigated in the wide-angle region where the three Mandelstam variables, s , $-t$ and $-u$, are much larger than Λ^2 . The constant Λ is a typical hadronic scale of order 1 GeV. In Eq. (1) q, p, p' denote the momenta of the involved particles and μ, ν, ν' their helicities. It is advantageous to work in a symmetric frame in which the skewness, ξ , defined by the following ratio of light-cone plus components of the baryon momenta

$$\xi = \frac{(p - p')^+}{(p + p')^+} \quad (2)$$

is zero. Except of baryon-mass corrections the particle momenta are parameterized as

$$\begin{aligned} p &= \left[p^+, -\frac{t}{8p^+}, -\frac{1}{2}\sqrt{-t}, 0 \right], \\ p' &= \left[p^+, -\frac{t}{8p^+}, \frac{1}{2}\sqrt{-t}, 0 \right], \\ q &= \left[q^+, -\frac{t}{8q^+}, \frac{1}{2}\sqrt{-t}, 0 \right], \end{aligned} \quad (3)$$

in light-cone coordinates where

$$p^+ = (\sqrt{s} + \sqrt{-u})/4, \quad q^+ = (\sqrt{s} - \sqrt{-u})/4. \quad (4)$$

The pion momentum is fixed by momentum conservation.

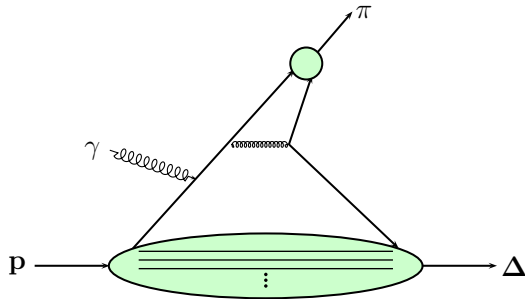


Figure 1: A typical graph for the handbag mechanism. The shaded regions are soft regions in which no hard scale appear.

In the handbag mechanism a (light-cone) helicity amplitude, $\mathcal{M}_{0\nu',\mu\nu}$, for the process (1) factorize in a product of subprocess amplitudes, \mathcal{H} , for pion photoproduction off quarks and form factors which represent the soft physics that controls the emission and reabsorption of quarks from the baryons, see Fig. 1. These form factors represent $1/x$ -moments of zero-skewness proton- Δ GPDs. The arguments for this type of factorization are presented in [6, 7] in detail. Thus, a brief repetition of the arguments should be enough: It is assumed that the parton virtualities are restricted by $k_i^2 < \Lambda^2$ and that the intrinsic transverse momenta, $k_{\perp i}$, defined with respect to their parent hadron's momentum, satisfy the condition $k_{\perp i}/x_i < \Lambda^2$ where x_i is the momentum fraction that parton i carries. One can then show that, up to corrections of order $\Lambda/\sqrt{-t}$, the subprocess Mandelstam variables, $\hat{s}, \hat{t}, \hat{u}$, coincide with the ones for the full process

$$\hat{t} = t, \quad \hat{s} = (k_j + q)^2 \simeq (p + q)^2 = s, \quad \hat{u} = (k'_j - q)^2 \simeq (p' - q)^2 = u, \quad (5)$$

where k_j and $k'_j = k_j + q - q'$ denote the momenta of the active partons, i.e. those partons to which the photon couple. Hence, the active partons are approximately on-shell, move collinear with their parent hadrons and carry momentum fractions close to unity, $x_j, x'_j \simeq 1$. As in deeply virtual exclusive scattering, the physical situation is that of a hard parton-level subprocess, $\gamma q_a \rightarrow \pi q_b$, and a soft emission and reabsorption of quarks from the baryons. Thus, up to corrections of order $\Lambda/\sqrt{-t}$, one can write a helicity amplitude for $\gamma p \rightarrow \pi \Delta$ as

$$\mathcal{M}_{0\nu',\mu\nu} = e_0 \int \frac{dx}{x} \sum_{\lambda',\lambda} \mathcal{H}_{0\lambda',\mu\lambda} A_{\nu'\lambda',\nu\lambda} \quad (6)$$

where λ and λ' denote the helicities of the emitted and reabsorbed quark and e_0 is the positron charge. The soft $p - \Delta$ matrix elements, A , of quark field operators are [13]

$$A_{\nu'\lambda',\nu\lambda} = \int \frac{z^-}{2\pi} e^{ixP^+z^-} \langle \Delta^{++}(p', \nu') | \mathcal{O}_{\lambda\lambda} | p(p, \nu) \rangle |_{z^+=0, z_\perp=0} \quad (7)$$

where

$$\begin{aligned} \mathcal{O}_{\lambda\lambda} &= \frac{1}{4} \bar{u}(-z/2) \gamma^+ (1 + 2\lambda\gamma_5) d(z/2), \\ \mathcal{O}_{-\lambda\lambda} &= -\frac{i\lambda}{2} \bar{u}(-z/2) (\sigma^{+1} - 2\lambda i\sigma^{+2}) d(z/2). \end{aligned} \quad (8)$$

These matrix elements describe the emission and of on-shell quarks with helicity λ and reabsorption of an on-shell quark with helicity λ' [16]. They are parameterized as $p - \Delta$ transition GPDs [3, 13] and are explicitly given in [13]. For wide-angle photoproduction only the matrix elements at zero skewness are needed. Nevertheless 14 of the altogether 16 $p - \Delta$ GPDs contribute at this value of skewness. Only the GPDs G_4 and \tilde{G}_4 and their associated form factors decouple.

For the process of interest there are three charge configurations in the final state: $\pi^- \Delta^{++}$, $\pi^0 \Delta^+$ and $\pi^+ \Delta^0$. The corresponding GPDs and their associated form factors are related by isospin symmetry [3]

$$G^{p\Delta^{++}}(x, t) = -\frac{\sqrt{3}}{2} G^{p\Delta^+}(x, t) = -\sqrt{3} G^{p\Delta^0}(x, t). \quad (9)$$

The skewness variable is omitted in the GPDs for convenience. One can also generalize the handbag mechanism to wide-angle electroproduction of $\pi\Delta$ final states provided that the photon virtuality, Q^2 , is less than $-t$ and $-u$. This calculation is analogous to the case of π -nucleon, see [9]. The photon virtuality affects only the subprocess amplitudes. The photoproduction of $\eta\Delta^+$ and $\eta'\Delta^+$ is a direct generalization of the calculation of η, η' -photoproduction [17]. Kaon- Σ^* production requires $p - \Sigma^*$ GPDs (with sd flavor content) which are related to the $p - \Delta$ GPDs (with du flavor content) by SU(3) flavor symmetry [3], e.g.

$$G_{p\Sigma^{*0}}^{sd} = \frac{1}{\sqrt{2}} G_{p\Delta^0}^{du}. \quad (10)$$

Otherwise the calculation of these processes is similar to the $\pi\Delta$ case investigated here. Finally, photoproduction of vector mesons at wide-angles can also be treated with the handbag mechanism [7]. However, for flavor-neutral vector mesons there is an additional gluonic subprocess, $\gamma g \rightarrow Vg$, which goes along with gluonic $p-\Delta$ transition GPDs and their corresponding form factors.

3 The subprocess

The amplitudes for the subprocess $\gamma q_a \rightarrow \pi q_b$ have been calculated in collinear factorization to twist-3 accuracy¹. At leading-order of perturbative QCD the twist-2 contribution reads [7, 8]

$$\begin{aligned} \mathcal{H}_{0\lambda\mu\lambda} &= \sqrt{2}\pi\alpha_s(\mu_R)\mathcal{C}_\pi^{(ab)}\frac{C_F}{N_C}\frac{f_\pi}{\sqrt{-\hat{t}}}\int_0^1\frac{d\tau}{\tau}\Phi_\pi(\tau,\mu_R) \\ &\times \left[(1+2\lambda\mu)\hat{s} - (1-2\lambda\mu)\hat{u}\right]\left(\frac{e_a}{\hat{s}} + \frac{e_b}{\hat{u}}\right) \end{aligned} \quad (11)$$

where the flavor weight factors are

$$\mathcal{C}_{\pi^+}^{ud} = \mathcal{C}_{\pi^-}^{du} = 1, \quad \mathcal{C}_{\pi^0}^{uu} = -\mathcal{C}_{\pi^0}^{dd} = \frac{1}{\sqrt{2}}. \quad (12)$$

All other \mathcal{C}_π^{ab} are zero. The strong coupling constant is evaluated in the one-loop approximation using the renormalization (and factorization) scale

$$\mu_R^2 = \mu_F^2 = \frac{\hat{t}\hat{u}}{\hat{s}}. \quad (13)$$

This scale takes care of the requirement that all Mandelstam variables should be large. Up to mass corrections $\mu_R^2 \simeq s/4$ for a c.m.s. scattering angle near 90° . For the familiar pion decay constant, f_π , the value 132 MeV is taken; $N_C (= 3)$ is the number of colors and $C_F = (N_C^2 - 1)/(2N_C)$. The quark charges, e_a and e_b , are given in units of the positron charge. Finally, ϕ_π is the twist-2 pion distribution amplitude for which the truncated Gegenbauer expansion is used

$$\phi_\pi(\tau, \mu_R) = 6\tau\bar{\tau} \left[1 + a_2(\mu_0)L^{\gamma_2/\beta_0}C_2^{3/2}(2\tau - 1)\right] \quad (14)$$

¹In the calculation of the subprocess amplitude as well as in the definition of the $p-\Delta$ matrix elements light-cone gauge is used.

with the lattice QCD result for the second Gegenbauer coefficient [18]

$$a_2(\mu_0) = 0.1364 \quad (15)$$

quoted at the initial scale $\mu_0 = 2$ GeV. The anomalous dimension is $\gamma_2 = 50/9$ and $\beta_0 = (11N_C - 2n_f)/3$ ($n_f = 4$). The quantity L is defined as

$$L = \frac{\alpha_s(\mu_R)}{\alpha_s(\mu_0)} = \frac{\ln(\mu_0^2/\Lambda_{\text{QCD}}^2)}{\ln(\mu_R^2/\Lambda_{\text{QCD}}^2)} \quad (16)$$

where the value $\Lambda_{\text{QCD}} = 0.22$ GeV is adopted. The τ -integration in (11) can be carried out analytically for the distribution amplitude (14):

$$\int_0^1 \frac{d\tau}{\tau} \phi_\pi(\tau, \mu_R) = 3[1 + a_2(\mu_R)]. \quad (17)$$

The twist-3 contribution has been calculated in [8, 9] and for details of this contribution it is referred to these papers. It consists of two parts - the 2-body one (the twist-3 $q\bar{q}$ Fock component of the pion with the distribution amplitudes $\phi_{\pi p}$ and $\phi_{\pi\sigma}$) and the 3-body one (the $q\bar{q}g$ Fock component with the distribution amplitude $\phi_{3\pi}$). Both contributions are related to each other by the equation of motion. In light-cone gauge the relations read

$$\begin{aligned} f_\pi \mu_\pi \left[\bar{\tau} \phi_{\pi p}(\tau) - \frac{\bar{\tau}}{6} \frac{d}{d\tau} \phi_{\pi\sigma}(\tau) - \frac{1}{3} \phi_{\pi\sigma}(\tau) \right] &= \\ & 2f_{3\pi} \int_0^{\bar{\tau}} \frac{d\tau_g}{\tau_g} \phi_{3\pi}(\tau, \bar{\tau} - \tau_g, \tau_g), \\ f_\pi \mu_\pi \left[\tau \phi_{\pi p}(\tau) + \frac{\tau}{6} \frac{d}{d\tau} \phi_{\pi\sigma}(\tau) - \frac{1}{3} \phi_{\pi\sigma}(\tau) \right] &= \\ & 2f_{3\pi} \int_0^\tau \frac{d\tau_g}{\tau_g} \phi_{3\pi}(\bar{\tau} - \tau_g, \bar{\tau}, \tau_g). \end{aligned} \quad (18)$$

The parameter μ_π appearing in (18) is defined as

$$\mu_\pi = \frac{m_\pi^2}{m_u + m_d}, \quad (19)$$

i.e. it is pion mass enhanced by the chiral condensate by means of the divergence of the axial-vector current (m_u and m_d are current quark masses). At the initial scale the value $\mu_\pi = 2$ GeV is taken. It evolves as

$$\mu_\pi(\mu_F) = L^{-4/\beta_0} \mu_\pi(\mu_0). \quad (20)$$

Because of the relations (18) the 2-body distribution amplitudes $\phi_{\pi p}$ and $\phi_{\pi\sigma}$ are not required explicitly although they are fixed by (18) for a given 3-body distribution amplitude, $\phi_{3\pi}$. Thus, the full twist-3 contribution to the subprocess amplitudes can solely be expressed by the 3-body distribution amplitude. As the twist-2 distribution amplitude the 3-body one is conventionally normalized to unity and accompanied by the normalization parameter $f_{3\pi}$ which is scale dependent and evolves as

$$f_{3\pi}(\mu_R) = L^{(16/3C_F-1)/\beta_0} f_{3\pi}(\mu_0). \quad (21)$$

The combined 2- and 3-body twist-3 amplitudes read [9]

$$\begin{aligned} \mathcal{H}_{0-\lambda\mu\lambda} &= 2\sqrt{2}\pi\alpha_s(\mu_R)\mathcal{C}_\pi^{(ab)}\frac{C_F}{N_C}f_{3\pi}(\mu_R)(2\lambda-\mu)\frac{\sqrt{-\hat{u}\hat{s}}}{\hat{s}^2\hat{u}^2} \\ &\times \int_0^1 d\tau \int_0^{\bar{\tau}} \frac{d\tau_g}{\tau_g} \Phi_{3\pi}(\tau, \bar{\tau} - \tau_g, \tau_g, \mu_R) \\ &\times \left[\left(\frac{1}{\bar{\tau}^2} - \frac{1}{\bar{\tau}(\bar{\tau} - \tau_g)} \right) (e_a \hat{u}^2 + e_b \hat{s}^2) - \frac{C_G}{C_F} \frac{2\hat{t}}{\tau\tau_g} (e_a \hat{u} + e_b \hat{s}) \right] \end{aligned} \quad (22)$$

where ($C_A = N_C$)

$$C_G = C_F - \frac{1}{2}C_A. \quad (23)$$

One directly sees from (22) that ²

$$\mathcal{H}_{0-++} = \mathcal{H}_{0+--} = 0, \quad \mathcal{H}_{0--+} = -\mathcal{H}_{0++-}. \quad (24)$$

Following [19] a truncated conformal expansion is used for the 3-body distribution amplitude

$$\begin{aligned} \Phi_{3\pi}(\tau_1, \tau_2, \tau_g, \mu_R) &= 360\tau_1\tau_2\tau_g^2 \left(1 + \omega_{10}(\mu_R)\frac{1}{2}(7\tau_g - 3) \right. \\ &+ \omega_{20}(\mu_R)(2 - 4\tau_1\tau_2 - 8\tau_g + 8\tau_g^2) \\ &+ \left. \omega_{11}(\mu_R)(3\tau_1\tau_2 - 2\tau_g + 3\tau_g^2) \right). \end{aligned} \quad (25)$$

The evolution of the expansion coefficients can be found in [9, 19]. Note that the coefficients ω_{20} and ω_{10} mix under evolution. For the distribution

²Explicit helicities of the subprocess amplitudes as well as of the full amplitudes, \mathcal{M} , are labeled by their signs. Those of the $\Delta(1232)$ are denoted by $2\nu'$.

amplitude (25) the integrals in (22) can be carried out analytically:

$$\begin{aligned}
\mathcal{H}_{0-\lambda\mu\lambda} &= -40\sqrt{2}\pi\alpha_s C_\pi^{(ab)} \frac{C_F}{N_C} f_{3\pi}(2\lambda - \mu) \frac{\sqrt{-\hat{u}\hat{s}}}{\hat{s}^2\hat{u}^2} \\
&\times \left[\left(1 - \frac{3}{16}\omega_{10} + \frac{6}{25}\omega_{20} - \frac{3}{50}\omega_{11}\right)(e_a\hat{u}^2 + e_b\hat{s}^2) \right. \\
&\left. + 6\frac{C_G}{C_F}\left(1 - \frac{5}{8}\omega_{10} + \frac{2}{5}\omega_{20} + \frac{1}{10}\omega_{11}\right)\hat{t}(e_a\hat{u} + e_b\hat{s}) \right]. \quad (26)
\end{aligned}$$

In [8] the following 3-body distribution amplitude has been used to fit the CLAS data [20] on π^0 photoproduction:

$$\begin{aligned}
f_{3\pi}(\mu_0) &= 0.004 \text{ GeV}^2, \\
\omega_{10}(\mu_0) &= -2.55, \quad \omega_{20}(\mu_0) = 8.0, \quad \omega_{11}(\mu_0) = 0. \quad (27)
\end{aligned}$$

The parameter $f_{3\pi}$ is taken from a QCD sum rules analysis and is subject to an uncertainty of about 30% [21].

Another 3-body distribution amplitude has been advocated for in [22]:

$$\begin{aligned}
f_{3\pi}(\mu_0) &= 0.004 \text{ GeV}^2, \\
\omega_{10}(\mu_0) &= 2.5, \quad \omega_{20}(\mu_0) = 6.0, \quad \omega_{11}(\mu_0) = 0. \quad (28)
\end{aligned}$$

This distribution amplitude leads to a fit to the CLAS photoproduction data of similar quality as (27) but, in contrast to (27), also to fair agreement with the data on deeply virtual pion electroproduction [23, 24, 25]. In earlier analyses [26, 27] of deeply virtual pion electroproduction the Wandzura-Wilczek approximation has been used, i.e. the 3-body twist-3 contribution has been neglected.

4 The GPDs in the large- N_C limit

As already mentioned there are 14 GPDs contributing to the photoproduction amplitudes and all of them are unknown at present. In order to achieve estimates of the cross section for the process of interest recourse will be taken to large- N_C results. In the limit of large N_C the nucleon and the $\Delta(1232)$ are different excitations of the chiral soliton and they are degenerated in mass. This leads to relations between proton- Δ^+ and proton-proton matrix

elements of quark-field operators. The following results for the $p - \Delta^{++}$ GPDs, defined in [3, 13] are to be found in the literature ³

$$G_1^{p\Delta^{++}} = \frac{3}{2}[E^u - E^d], \quad [3]$$

$$\tilde{G}_3^{p\Delta^{++}} = -\frac{3}{2}[\tilde{H}^u - \tilde{H}^d], \quad [14]$$

$$G_{T5}^{p\Delta^{++}} + \frac{1}{2}G_{T7}^{p\Delta^{++}} = -\frac{3}{2}[H_T^u - H_T^d]. \quad [13] \quad (29)$$

If all other transition GPDs and their associated form factors are neglected there are only four form factors contributing to wide-angle photoproduction of $\pi^- \Delta^{++}$:

$$\begin{aligned} R_1(t) &= \frac{3}{2} \int_0^1 \frac{dx}{x} [E^u(x, t) - E^d(x, t)], \\ \tilde{R}_3(t) &= -\frac{3}{2} \int_0^1 \frac{dx}{x} [\tilde{H}^u(x, t) - \tilde{H}^d(x, t)], \\ S_T(t) &= -\frac{3}{2} \int_0^1 \frac{dx}{x} [H_T^u(x, t) - H_T^d(x, t)], \end{aligned} \quad (30)$$

According to (29) $S_T = S_{T5} + S_{T7}/2$. In order to split S_T in S_{T5} and S_{T7} a parameter ϱ is introduced such that

$$S_{T5} = (1 - \varrho)S_T, \quad S_{T7} = 2\varrho S_T. \quad (31)$$

The parameter ϱ is varied between 0 and 1. This avoids a change of the sign of the form factors. A possible t -dependence of ϱ is ignored. Under these conditions the process amplitudes (6) read ⁴

$$\mathcal{M}_{03, \mu+} = \frac{e_0}{\sqrt{2}} \left(\frac{\sqrt{-t}}{2m} \sum_{\lambda} \mathcal{H}_{0\lambda, \mu\lambda} R_1 - \mathcal{H}_{0-, -\mu+} S_{T7} \right),$$

³In [3] the large- N_C relation for G_1 is quoted as

$$G_1^{p\Delta^{++}} = 3/2[H^u - H^d + E^u - E^d].$$

However, the contribution from H is suppressed by $1/N_C$ compared to E [28] and therefore neglected here.

⁴In principle there is also a contribution from the pion pole which can be neglected in the wide-angle region because the pole at $t = m_\pi^2$ is far away (m_π denotes the mass of the pion).

$$\begin{aligned}
\mathcal{M}_{01,\mu+} &= \frac{e_0}{2\sqrt{6}} \frac{1}{mM} \sum_{\lambda} \mathcal{H}_{0\lambda,\mu\lambda} (tR_1 + 2\lambda m(M+m)\tilde{R}_3) \\
&\quad - \frac{e_0}{2\sqrt{6}} \frac{\sqrt{-t}}{M} \left(\sum_{\lambda} \mathcal{H}_{0-\lambda,\mu\lambda} S_{T5} - 2\mathcal{H}_{0-,-\mu+} S_{T7} \right), \\
\mathcal{M}_{0-1,\mu+} &= \frac{e_0}{2\sqrt{6}} \frac{\sqrt{-t}}{M} \sum_{\lambda} \mathcal{H}_{0\lambda,\mu\lambda} (R_1 - 2\lambda \tilde{R}_3) \\
&\quad - \frac{e_0}{\sqrt{6}} \frac{m}{M} \mathcal{H}_{0-,\mu+} \left(\frac{M+m}{m} S_{T5} + S_{T7} \right), \\
\mathcal{M}_{0-3,\mu+} &= 0.
\end{aligned} \tag{32}$$

The proton and the $\Delta(1232)$ masses are denoted by m and M , respectively. The amplitudes for negative proton helicity follow from from parity invariance

$$\mathcal{M}_{0-\nu',-\mu-\nu} = (-1)^{\mu-\nu+\nu'} \mathcal{M}_{0\nu',\mu\nu}. \tag{33}$$

A flavor symmetric sea is assumed for the proton. Therefore, the isovector combination of a proton-proton GPD, $K_i^u - K_i^d$, is equal to the difference of the u and d valence-quark GPDs. The latter are parameterized as [29, 30]

$$K_i^a(x, t) = k_i^a(x) \exp [t f_i^a(x)] \tag{34}$$

for flavor a . The profile function reads

$$f_i^a(x) = (B_i^a - \alpha_i^a \ln x)(1-x)^3 + A_i^a x(1-x)^2. \tag{35}$$

This is a generalization to the large $-t$ region of the Regge-like parameterization frequently used in the analysis of deeply virtual exclusive processes. An important property of this profile function is the strong $x-t$ correlation: large (small) x go together with large (small) $-t$. It should be noted that the handbag mechanism probes the GPDs (34) at large x since it applies to large $-t$. In this region where the active parton carries most of the proton's momentum while all spectators are soft. This is the region of the Feynman mechanism. The parameters of the profile functions for the three relevant proton-proton GPDs are compiled in Tab. 1.

The forward limit of \tilde{H} is given by the polarized parton densities

$$\tilde{h}^a(x) = \Delta q^a(x) \tag{36}$$

which are taken from [31]. That of H_T is related the transversity distribution. Following an ansatz proposed in [32], h_T is parameterized as [27]

$$h_T^a(x) = N_T^a \sqrt{x}(1-x)[q^a(x) + \Delta q^a(x)]. \quad (37)$$

With this parameterization the Soffer bound is respected. The unpolarized parton densities, $q^a(x)$, are taken from [33]. The normalization N_T^a is [27]

$$N_T^u = 1.1, \quad N_T^d = -0.3. \quad (38)$$

In contrast to the H -type GPDs the forward limit of E is not accessible in deep inelastic electron-proton scattering. Therefore, it is parameterized analogously to the parton densities but with new parameters which are fixed in an analysis of the electromagnetic form factors of the nucleon performed by [30]

$$e^a(x) = \kappa_a N_a x^{-\alpha_a} (1-x)^{\beta_a} (1 + \gamma_a \sqrt{x}). \quad (39)$$

The normalization N_a ensures

$$\int_0^1 dx e_a(x) = \kappa_a. \quad (40)$$

The quantity κ_a is the contribution of quarks with flavor a to the anomalous magnetic of the proton. Its value is computed from the anomalous magnetic moments of the proton and neutron: $\kappa_u = 1.67$, $\kappa_d = -2.03$. The other parameters in(39) are [30]:

$$\begin{aligned} \alpha_u &= 0.603, & \alpha_d &= 0.603, \\ \beta_u &= 4.65, & \beta_d &= 5.25, \\ \gamma_u &= 4, & \gamma_d &= 0. \end{aligned} \quad (41)$$

In Fig. 2 the $p - \Delta^{++}$ form factors are displayed. The error bands are those of the corresponding proton-proton form factors, see [8, 30].

The mentioned zero-skewness proton-proton GPDs have been extracted and used in analyses of the electromagnetic and axial form factors of the nucleon, wide-angle Compton scattering and pion photoproduction. With the skewness dependence generated through double distributions [39] they have also been applied in analyses of deeply virtual exclusive processes. Another test of the GPDs is provided by the magnetic $p - \Delta^*$ transition form factor, G_M^* , for which data are available at fairly large values of $-t$ [35, 36, 37], see

Table 1: The parameters of the profile functions. Those for the valence-quark GPD E are taken from [30], for \widetilde{H} from [34] and for H_T from [8].

	E^u	E^d	\widetilde{H}^u	\widetilde{H}^d	H_T^u	H_T^d
$\alpha'[\text{GeV}^{-2}]$	0.961	0.861	0.432	0.387	0.45	0.45
$B[\text{GeV}^{-2}]$	0.333	-0.635	0.654	0.400	0.3	0.3
$A[\text{GeV}^{-2}]$	1.187	3.106	1.239	4.284	0.5	0.5

Fig. 3. The experimental value of $G_M^*(0)$ has been extracted from the MAMI data [38] on the $\gamma N\Delta$ amplitudes at the resonance position [40]:

$$G_M^*(0) = 3.02 \pm 0.03. \quad (42)$$

In the large- N_C limit G_M^* is related to the proton-proton GPD E by [3]

$$\begin{aligned} G_M^*(t) &= -\frac{1}{3} \int_0^1 dx G_1^{p\Delta^+}(x, t) = \frac{1}{\sqrt{3}} \int_0^1 dx [E^u(x, t) - E^d(x, t)] \\ &= \frac{1}{\sqrt{3}} [F_2^u(t) - F_2^d(t)] \end{aligned} \quad (43)$$

where F_2^a denotes the flavor- a Pauli form factor of the nucleon. At $t = 0$ in particular one obtains from (43)

$$G_M^*(0) = \frac{1}{\sqrt{3}} (\kappa_u - \kappa_d) = 2.14. \quad (44)$$

This value of $G_M^*(0)$ is too small by about 30%. Errors of this size are to be expected for large N_C results ⁵. In order to test the t -dependence of the large- N_C prediction, we follow [42] and normalize the magnetic transition form factor G_M^* to the experimental value (42):

$$G_M^*(t) = \frac{3.02}{\kappa_u - \kappa_d} [F_2^u(t) - F_2^d(t)] \quad (45)$$

⁵Taking into account corrections suppressed by $1/N_C$ compared to (43), one obtains $G_M^*(0) = 2.71$ and for the magnetic moment $\mu_{p\Delta^+} = (\mu_p - \mu_n)/\sqrt{2}$ [3, 41].

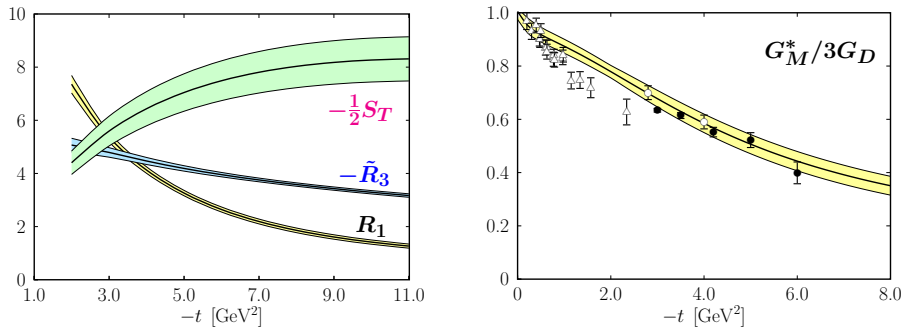


Figure 2: (Left) The proton- Δ^{++} form factors in the large- N_C limit scaled by t^2 versus $-t$. The shaded bands indicate the uncertainties of the corresponding proton-proton form factors.

Figure 3: (Right) The magnetic $p - \Delta^+$ transition form factor G_M^* scaled by three times the dipole form factor $G_D = (1 - t/0.71 \text{ GeV}^2)^{-2}$ versus $-t$. The shaded band represents the uncertainty of the prediction. Data are taken from [35, 36, 37].

In Fig. 3 the experimental data on the magnetic $p - \Delta^+$ form factor G_M^* are compared with the large- N_C predictions computed from the GPD E respective the flavor Pauli form factors proposed in [30]. For $-t$ less than 2 GeV^2 there are some discrepancies with the data of [35]. On the other hand, for $-t$ larger than about 2 GeV^2 - this is the region relevant in this work - there is good agreement with experiment, i.e. the t -dependence of G_M^* is well in agreement with the large- N_C prediction. That the large- N_C relation between the GPDs G_1 and E (see Eq. (29)) implies similar shapes of the Pauli form factor and G_M^* has already been noticed by Stoler [43].

The parameterization (34) of the GPDs with the profile function (35) has a remarkable property: As shown in [29] the moments of the GPDs behave power-law like at large $-t$. The power is controlled by the power β_i of the factor $1 - x$ that characterizes the behavior of a GPD K_i for $x \rightarrow 1$. Thus, for instance

$$F_2^a \sim (-t)^{-d_e^a} \quad (46)$$

with $d_e^a = (1 + \beta_e^a)/2$. For the Pauli form factor the powers are [30]

$$d_e^u = 2.83, \quad d_e^d = 3.12. \quad (47)$$

As is to be seen from Fig. 3 G_M^* falls faster than $1/t^2$ and seems to be in

agreement with the dominance of the GPD E . Since the valence quark densities behave about as $(1-x)^{3.4}$ for $x \rightarrow 1$ for u -quarks [30] and a somewhat stronger fall-off for d -quarks, the u -quark contribution dominates the form factors \tilde{R}_3, S_{T5} and S_{T7} at large $-t$. Hence, the form factor \tilde{R}_3 falls approximately as $(-t)^{-2.2}$ and S_{T5}, S_{T7} as $(-t)^{-2.7}$. This power-law behavior of the GPD-moments obtained with the profile function (35) is to be contrasted with the familiar Regge-like profile function, i.e. $A_i = 0$ in (35), which leads to exponentially decreasing GPD moments. The powers β_i extracted from parton densities or from electromagnetic form factors [30] are to be considered as effective powers since they are fixed in regions of x less than about 0.8. They are likely subject to change as soon as data sensitive to larger x become available. It is well possible that at last the powers agree with the theoretical expectations for $x \rightarrow 1$ [44], e.g. ($a = u, d$)

$$H^a \sim (1-x)^3, \quad E^a \sim (1-x)^5. \quad (48)$$

5 Observables, predictions and comparison with experiment

Now, having specified the distribution amplitudes and the form factors, we are in the position to compute the amplitudes (32) and subsequently the differential cross section for $\pi\Delta$ photoproduction

$$\frac{d\sigma}{dt} = \frac{1}{32\pi(s-m^2)^2} \sum_{\nu'\mu} |\mathcal{M}_{0\nu',\mu+}|^2. \quad (49)$$

In Figs. 4 and 5 the predictions for the $\pi^-\Delta^{++}$ cross section, scaled by s^7 , are shown at two values of s and compared with the available data [15]. The cross section is displayed versus the cosine of the c.m.s. scattering angle θ . The predictions are evaluated from the 3-body distribution amplitude (28) and ϱ is fitted to the data. Fair agreement with experiment is obtained for $\varrho = 1.0$ (i.e. $S_{T5} = 0, S_{T7} = 2S_T$). It is to be stressed that this is the only parameter that is fitted to the data. All other input functions, distribution amplitudes and GPDs, are fixed in studies of deeply virtual and wide-angle processes with exclusive photon- and meson-nucleon final states [8, 9, 22, 26, 27, 34, 45] as well as in the analysis of the electromagnetic form factors [30]. The dependence of the predicted cross section on the value of ϱ is

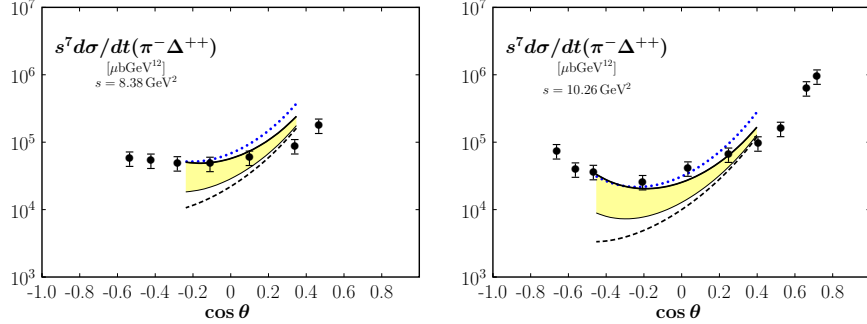


Figure 4: (Left) The differential cross section for $\pi^-\Delta^{++}$, scaled by s^7 , at $s = 8.38 \text{ GeV}^2$ versus $\cos\theta$. The solid (dashed, dotted) line is evaluated from $\varrho = 1.0$ and the distribution amplitude (28) (the twist-2 contribution, $\pi^+\Delta^0$). The shaded band represents the dependence on ϱ varying it between 0 and 1. Theoretical results are only shown for $-t$ and $-u$ larger than 2.5 GeV^2 . Data is taken from [15].

Figure 5: (Right) As Fig. 4 but for $s = 10.26 \text{ GeV}^2$.

shown as a shaded band in Fig. 4. This dependence constitutes a substantial part of the uncertainties of the predictions. For the parameter $A_T^u = A_T^d$ in the profile function of the GPD H_T the value 0.5 GeV^{-2} is chosen as in [8, 9]. It is not well constrained by the available data on photoproduction of πN and $\pi\Delta$ states [15, 20], it can be varied between 0.3 and 0.7 GeV^{-2} . It should also be mentioned that the theoretical results are only shown for $-t$ and $-u$ larger than 2.5 GeV^2 in order to meet approximately the requirement of the handbag mechanism that the Mandelstam variables should be (much) larger than a typical hadronic scale of order 1 GeV^2 . Baryon-mass corrections have been studied in [46] by testing other possibilities to assign the subprocess Mandelstam variables to the full ones than (5). According to [46] the mass corrections are not small at $s \simeq 10 \text{ GeV}^2$.

In the figures the twist-2 contribution is separately shown. It dominates in the forward hemisphere whereas in the backward region the twist-3 contributions takes the lead. This is also the case for photoproduction of charged pions and nucleons [9]. In contrast to the latter processes the $\pi^+\Delta^0$ cross section is larger than the $\pi^-\Delta^{++}$ one in the forward hemisphere (at $s = 10.26 \text{ GeV}^2$ about a factor of 1.7 at $\cos\theta \simeq 0.4$, slightly increasing with energy) but becomes a little bit smaller in the backward hemisphere (about

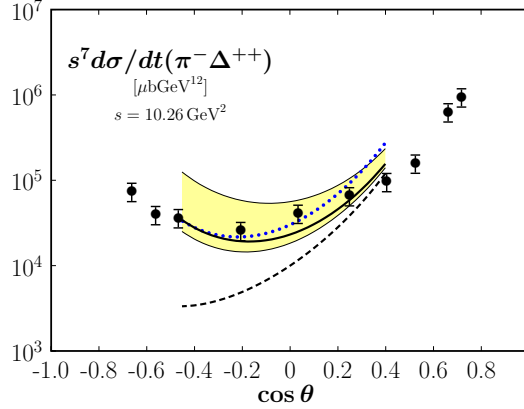


Figure 6: The scaled $\pi^-\Delta^{++}$ differential cross section at $s = 10.26 \text{ GeV}^2$. The solid (dashed, dotted) line is evaluated from the distribution amplitude (27) and the assumption $\varrho = 0.2$ (the twist-2 contribution, $\pi^+\Delta^0$). For other notations it is referred to Fig. 4.

a factor of 0.95 at $\cos \theta \simeq -0.4$) although the subprocess amplitudes for π^- production are larger than those for π^+ (see Eq. (22))

$$\frac{\mathcal{H}^{\pi^-}}{\mathcal{H}^{\pi^+}} \sim \left| \frac{e_d \hat{u}^n + e_u \hat{s}^n}{e_u \hat{u}^n + e_d \hat{s}^n} \right| \quad (50)$$

($n = 1, 2$). The larger π^+ cross section is caused by the factor $\sqrt{3}$ in the isospin relation (9).

In Fig. 6 the cross section evaluated from the distribution amplitude (27) together with $\varrho = 0.2$ (in this case $S_{T5} = 2S_{T7}$) is shown at $s = 10.26 \text{ GeV}^2$. The properties of the predictions evaluated from this distribution amplitude are very similar to the scenario discussed above. Also their energy dependency is similar. It is to be stressed that the distribution amplitudes (27) and (28) lead to similar results for $\gamma p \rightarrow \pi^0 p$ in the wide-angle region but to very different results for deeply virtual pion electroproduction [22]. The reason for that difference lies in the fact that to deeply virtual pion electroproduction there is also a strong contribution from the 2-body twist-2 distribution amplitude, $\phi_{\pi p}$, which is fixed by the 3-body twist-3 distribution amplitude via the equation of motion. The 3-body distribution amplitude (25) leads to

$$\phi_{\pi p}(\tau) = 1 + \frac{f_{3\pi}}{f_\pi \mu_\pi} \omega(1 - 30\tau^2 \bar{\tau}^2) \quad (51)$$

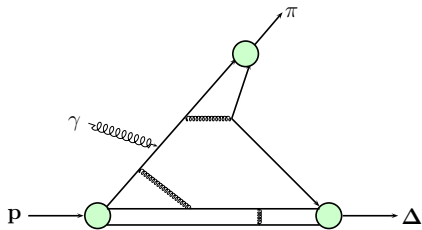


Figure 7: A typical graph for the hard perturbative mechanism [47, 48]. The shaded regions are soft regions in which no hard scale occur.

where

$$\omega = 7\omega_{10} - 2\omega_{20} - \omega_{11}. \quad (52)$$

From the distribution amplitude (27) one finds $\omega(\mu_0) = -33.85$ whereas (28) leads to $\omega(\mu_0) = 5.5$. The different values of ω have a strong impact on the results for electroproduction.

A comparison of the cross sections at $s = 8.38$ and 10.26 GeV^2 reveals that the handbag results do not scale as s^{-7} . This would only happen for a dominant twist-2 contribution and if the form factor R_1 would drop as $1/t^3$ and \tilde{R}_3 as $(-t)^{-2.5}$ which is not the case, see the discussion at the end of Sect. 4. The twist-3 contribution scales as s^{-8} (if $S_T \sim (-t)^{-2.5}$). Moreover, there is a number of logarithms generated by the evolution of the distribution amplitudes and GPDs. Thus, effectively the handbag result for the cross section scales about as $s^{-9.5}$. A possible evolution of the form factors which - as said - represent $1/x$ -moments of GPDs, is ignored. This is to some extent justified: At large $-t$ the form factors are accumulated in a narrow range of large x , see (34), (35). Because of the strong $x - t$ correlation of the GPDs this range of x approaches 1 and becomes narrower for increasing $-t$. Therefore, for very large $-t$ the form factors approximately become equal to the scale-independent lowest moments of the GPDs. One may argue that the disregard of the GPD evolution also requires the neglect of the scale-dependence of the distribution amplitudes for consistency. Thus, as an example, the cross section is evaluated from the distribution amplitude (28) taken at the fixed scale $\mu_F = \mu_R = 1 \text{ GeV}$ and with $\varrho = 0.4$. The result agrees also reasonable well with experiment but, as expected, shows a milder energy dependence. Lack of data prevent a serious check of the energy dependence.

There is an alternative mechanism for wide-angle scattering [47, 48] for which, in contrast to the handbag mechanism, all partons inside the baryons participate in the hard process by the exchange of hard gluons. The dominant contribution in this case comes from the valence Fock component where the number of exchanged gluons is minimal, see Fig. 7. In the handbag mechanism, on the other hand, there is only one active parton, all others are spectators and it is summed over all Fock states, see Fig. 1. However, a calculation of $\gamma p \rightarrow \pi^- \Delta^{++}$ in the hard perturbative mechanism fails by about three orders of magnitude at $\theta \simeq 90^\circ$ [49].

Data on spin-dependent observables would give detailed information on the various $p - \Delta$ transition GPDs. Such observables could be measured with polarized photons and protons. The spin density matrix elements of the $\Delta(1232)$ would provide further information on the GPDs. At present just four out of 14 GPDs are fixed by the large- N_C relations (29), the others are assumed to be zero. This scenario is probably inadequate to explain all spin phenomena. Thus, likely, the large- N_C GPDs (29) do not allow reliable predictions of spin-dependent observables. An exception is perhaps the correlation of the photon and proton helicities, A_{LL} , which like the cross section, only depends on the absolute values of the amplitudes:

$$\begin{aligned} A_{LL} &= \frac{d\sigma(++)-d\sigma(-+)}{d\sigma(++)+d\sigma(-+)} \\ &= \frac{\sum_{\nu'} [|\Phi_{0\nu',++}|^2 - |\Phi_{0\nu',-+}|^2]}{\sum_{\nu'} [|\Phi_{0\nu',++}|^2 + |\Phi_{0\nu',-+}|^2]} \end{aligned} \quad (53)$$

where $d\sigma(\mu\nu)$ is the cross section with definite initial state helicities. The amplitudes Φ are standard c.m.s. helicity amplitudes which are more convenient for the treatment of spin-dependent observables than the light-cone helicity amplitudes. The amplitudes Φ can be obtained from the light-cone helicity amplitudes \mathcal{M} (32) which naturally appear in the handbag mechanism, by using the transform from light-cone spinors to ordinary spinors given in [16]. This transform generates corrections to a given helicity amplitude $\Phi_{0\nu',\mu+} \approx \mathcal{M}_{0\nu',\mu+}$ of order

$$\eta_0 = \frac{2\sqrt{-t}}{\sqrt{s} + \sqrt{-u}} \frac{M(m)}{\sqrt{s}} \quad (54)$$

from other light-cone helicity amplitudes.

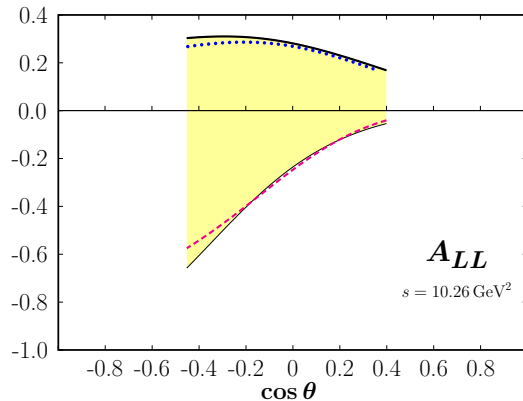


Figure 8: The helicity correlation parameters A_{LL} at $s = 10.26 \text{ GeV}^2$. The solid (dotted) line is evaluated from the distribution amplitude (28) and $\varrho = 1.0$ for $\pi^- \Delta^{++}$ ($\pi^+ \Delta^0$). The dashed line is computed from the distribution amplitude (27) and $\varrho = 0.2$. For other notations it is referred to Fig. 4.

Predictions of A_{LL} are displayed in Fig. 8. The results for the $\pi^- \Delta^{++}$ and $\pi^+ \Delta^0$ channels are evaluated from the distribution amplitude (28) and $\varrho = 1.0$. They are very similar, about 0.2. The distribution amplitude (27) (with $\varrho = 0.2$) leads to a negative A_{LL} .

6 Summary

Wide-angle photoproduction of $\pi \Delta(1232)$ final states at large energies is calculated within the handbag mechanism in which the process amplitudes factorize in hard partonic subprocess amplitudes and soft form factors representing $1/x$ -moments of zero-skewness $p - \Delta$ transition GPDs. The subprocess $\gamma q_a \rightarrow \pi q_b$ is the same as in pion photoproduction. The corresponding amplitudes have been calculated in [8] to twist-3 accuracy and to leading-order of perturbative QCD. The results given in [8] are used here. The $p - \Delta$ transition GPDs are related to the proton-proton GPDs in the large- N_C limit. The latter GPDs are known from analyses of the electromagnetic form factors, wide-angle Compton scattering and pion photoproduction as well as from investigations of deeply virtual meson production. There is only one issue that implies an unknown parameter: In the large- N_C limit only the sum of transversity GPDs $S_{T5} + 1/2 S_{T7}$ is related to a proton-proton

GPD. The splitting of the relation (29) into S_{T5} and S_{T7} is done with the help of a parameter ϱ (see (31)) which is fitted to the experimental data on $\gamma p \rightarrow \pi^- \Delta^{++}$ [15]. Reasonable agreement with experiment is achieved that way for two different 3-body twist-3 distribution amplitudes. These distribution amplitudes also lead to similar results for pion photoproduction but to very different results for deeply virtual electroproduction of pions [22]. A remeasurement of the cross section seems to be advisable since the SLAC data [15] are very old. Data at higher energies as well as spin-dependent data would be welcome. The handbag mechanism also applies to other photoproduction channels like $\eta\Delta^+$, $\rho\Delta$ or kaon- Σ^* but there are no data available for these processes at present.

References

- [1] X. D. Ji, Phys. Rev. D **55**, 7114-7125 (1997) [arXiv:hep-ph/9609381 [hep-ph]].
- [2] J. C. Collins, L. Frankfurt and M. Strikman, Phys. Rev. D **56**, 2982-3006 (1997) [arXiv:hep-ph/9611433 [hep-ph]].
- [3] A. V. Belitsky and A. V. Radyushkin, Phys. Rept. **418**, 1-387 (2005) [arXiv:hep-ph/0504030 [hep-ph]].
- [4] M. Diehl, Phys. Rept. **388**, 41-277 (2003) [arXiv:hep-ph/0307382 [hep-ph]].
- [5] A. V. Radyushkin, Phys. Rev. D **58**, 114008 (1998) [arXiv:hep-ph/9803316 [hep-ph]].
- [6] M. Diehl, T. Feldmann, R. Jakob and P. Kroll, Eur. Phys. J. C **8**, 409-434 (1999) [arXiv:hep-ph/9811253 [hep-ph]].
- [7] H. W. Huang and P. Kroll, Eur. Phys. J. C **17**, 423-435 (2000) [arXiv:hep-ph/0005318 [hep-ph]].
- [8] P. Kroll and K. Passek-Kumerički, Phys. Rev. D **97**, no.7, 074023 (2018) [arXiv:1802.06597 [hep-ph]].
- [9] P. Kroll and K. Passek-Kumerički, Phys. Rev. D **104**, no.5, 054040 (2021) [arXiv:2107.04544 [hep-ph]].

- [10] M. Burkardt, *Int. J. Mod. Phys. A* **18**, 173-208 (2003) [arXiv:hep-ph/0207047 [hep-ph]].
- [11] S. Diehl, K. Joo, K. Semenov-Tian-Shansky, C. Weiss, V. Braun, W. C. Chang, P. Chatagnon, M. Constantinou, Y. Guo and P. T. P. Hutaauruk, *et al.* [arXiv:2405.15386 [hep-ph]].
- [12] S. Diehl *et al.* [CLAS], *Phys. Rev. Lett.* **131**, no.2, 021901 (2023) doi:10.1103/PhysRevLett.131.021901 [arXiv:2303.11762 [hep-ex]].
- [13] P. Kroll and K. Passek-Kumerički, *Phys. Rev. D* **107**, no.5, 054009 (2023) [arXiv:2211.09474 [hep-ph]].
- [14] L. L. Frankfurt, M. V. Polyakov, M. Strikman and M. Vanderhaeghen, *Phys. Rev. Lett.* **84**, 2589-2592 (2000) [arXiv:hep-ph/9911381 [hep-ph]].
- [15] R. L. Anderson, D. Gustavson, D. Ritson, G. A. Weitsch, H. J. Halpern, R. Prepost, D. H. Tompkins and D. E. Wiser, *Phys. Rev. D* **14**, 679 (1976)
- [16] M. Diehl, *Eur. Phys. J. C* **19**, 485-492 (2001) [arXiv:hep-ph/0101335 [hep-ph]].
- [17] P. Kroll and K. Passek-Kumerički, *Phys. Rev. D* **105**, no.3, 034005 (2022) [arXiv:2111.08965 [hep-ph]].
- [18] V. M. Braun, S. Collins, M. Göckeler, P. Pérez-Rubio, A. Schäfer, R. W. Schiel and A. Sternbeck, *Phys. Rev. D* **92**, no.1, 014504 (2015) [arXiv:1503.03656 [hep-lat]].
- [19] V. M. Braun and I. E. Filyanov, *Z. Phys. C* **48**, 239-248 (1990).
- [20] M. C. Kunkel *et al.* [CLAS], *Phys. Rev. C* **98**, no.1, 015207 (2018) [arXiv:1712.10314 [hep-ex]].
- [21] P. Ball, *JHEP* **01**, 010 (1999) [arXiv:hep-ph/9812375 [hep-ph]].
- [22] G. Duplančić, P. Kroll, K. Passek-K. and L. Szymanowski, *Phys. Rev. D* **109**, no.3, 034008 (2024) [arXiv:2312.13164 [hep-ph]].
- [23] I. Bedlinskiy *et al.* [CLAS], *Phys. Rev. C* **90**, no.2, 025205 (2014) [arXiv:1405.0988 [nucl-ex]].

- [24] M. Dlamini *et al.* [Jefferson Lab Hall A], Phys. Rev. Lett. **127**, no.15, 152301 (2021) [arXiv:2011.11125 [hep-ex]].
- [25] M. G. Alexeev *et al.* [COMPASS], Phys. Lett. B **805**, 135454 (2020) [arXiv:1903.12030 [hep-ex]].
- [26] S. V. Goloskokov and P. Kroll, Eur. Phys. J. C **65**, 137-151 (2010) [arXiv:0906.0460 [hep-ph]].
- [27] S. V. Goloskokov and P. Kroll, Eur. Phys. J. A **47**, 112 (2011) [arXiv:1106.4897 [hep-ph]].
- [28] P. Schweitzer and C. Weiss, Phys. Rev. C **94**, no.4, 045202 (2016) [arXiv:1606.08388 [hep-ph]].
- [29] M. Diehl, T. Feldmann, R. Jakob and P. Kroll, Eur. Phys. J. C **39**, 1-39 (2005) [arXiv:hep-ph/0408173 [hep-ph]].
- [30] M. Diehl and P. Kroll, Eur. Phys. J. C **73**, no.4, 2397 (2013) [arXiv:1302.4604 [hep-ph]].
- [31] D. de Florian, R. Sassot, M. Stratmann and W. Vogelsang, Phys. Rev. D **80**, 034030 (2009) [arXiv:0904.3821 [hep-ph]].
- [32] M. Anselmino, M. Boglione, U. D'Alesio, A. Kotzinian, F. Murgia, A. Prokudin and C. Turk, Phys. Rev. D **75**, 054032 (2007) [arXiv:hep-ph/0701006 [hep-ph]].
- [33] J. Pumplin, D. R. Stump, J. Huston, H. L. Lai, P. M. Nadolsky and W. K. Tung, JHEP **07**, 012 (2002) [arXiv:hep-ph/0201195 [hep-ph]].
- [34] P. Kroll, Eur. Phys. J. A **53**, no.6, 130 (2017) [arXiv:1703.05000 [hep-ph]].
- [35] W. Bartel, B. Dudelzak, H. Krehbiel, J. McElroy, U. Meyer-Berkhout, W. Schmidt, V. Walther and G. Weber, Phys. Lett. B **28**, 148-151 (1968)
- [36] V. V. Frolov, G. S. Adams, A. Ahmidouch, C. S. Armstrong, K. Assamagan, S. Avery, O. K. Baker, P. E. Bosted, V. Burkert and R. Carlini, *et al.* Phys. Rev. Lett. **82**, 45-48 (1999) [arXiv:hep-ex/9808024 [hep-ex]].

- [37] M. Ungaro *et al.* [CLAS], Phys. Rev. Lett. **97**, 112003 (2006) [arXiv:hep-ex/0606042 [hep-ex]].
- [38] R. Beck, H. P. Krahn, J. Ahrens, J. R. M. Annand, H. J. Arends, G. Audit, A. Braghieri, N. d'Hose, D. Drecshel and O. Hanstein, *et al.* Phys. Rev. C **61**, 035204 (2000) [arXiv:nucl-ex/9908017 [nucl-ex]].
- [39] . V. Musatov and A. V. Radyushkin, Phys. Rev. D **61**, 074027 (2000) [arXiv:hep-ph/9905376 [hep-ph]].
- [40] L. Tiator, D. Drechsel, O. Hanstein, S. S. Kamalov and S. N. Yang, Nucl. Phys. A **689**, 205-214 (2001) [arXiv:nucl-th/0012046 [nucl-th]].
- [41] E. E. Jenkins and A. V. Manohar, Phys. Lett. B **335**, 452-459 (1994) [arXiv:hep-ph/9405431 [hep-ph]].
- [42] V. Pascalutsa, M. Vanderhaeghen and S. N. Yang, Phys. Rept. **437**, 125-232 (2007) [arXiv:hep-ph/0609004 [hep-ph]].
- [43] P. Stoler, Phys. Rev. Lett. **91**, 172303 (2003) [arXiv:hep-ph/0210184 [hep-ph]].
- [44] F. Yuan, Phys. Rev. D **69**, 051501 (2004) [arXiv:hep-ph/0311288 [hep-ph]].
- [45] S. V. Goloskokov and P. Kroll, Eur. Phys. J. C **53**, 367-384 (2008) [arXiv:0708.3569 [hep-ph]].
- [46] M. Diehl, T. Feldmann, H. W. Huang and P. Kroll, Phys. Rev. D **67**, 037502 (2003) [arXiv:hep-ph/0212138 [hep-ph]].
- [47] G. P. Lepage and S. J. Brodsky, Phys. Rev. D **22**, 2157 (1980).
- [48] A. V. Efremov and A. V. Radyushkin, Phys. Lett. B **94**, 245-250 (1980).
- [49] G. R. Farrar, K. Huleihel and H. Y. Zhang, Nucl. Phys. B **349**, 655-674 (1991).